New Ferrimagnetic Oxide $CaCu_3Cr_2Sb_2O_{12}$: High-Pressure Synthesis, Structure, and Magnetic Properties

Song-Ho Byeon,*,† Seoung-Soo Lee,† John B. Parise,*,‡ Patrick M. Woodward,§ and Nam Hwi Hur||

College of Environment and Applied Chemistry, Kyung Hee University, Kyung Ki 449-701, Korea, Department of Geosciences and Mineral Physics Institute, State University of New York, Stony Brook, New York 11794-2100, The Ohio State University, Department of Chemistry, Columbus, Ohio 43210-1185, and Center for CMR Materials, KRISS, Taejon 305-600, Korea

Received February 21, 2005. Revised Manuscript Received April 29, 2005

A new perovskite-type oxide, $CaCu_3Cr_2Sb_2O_{12}$, has been synthesized at 10 GPa and 1100 °C. This compound crystallizes in space group $Pn\bar{3}$ and shows simultaneous cation ordering on both A and B sites. Magnetization measurements indicate that an interaction between A-site Cu(II) and B-site Cr(III) cations dominates over possible antiferromagnetic couplings between Cu(II)−Cu(II) ions or Cr(III)−Cr(III) ions and induces net spontaneous magnetic moment below ∼160 K. The lack of significant hysteresis in the isothermal magnetization curves suggests that $CaCu_3Cr_2Sb_2O_{12}$ is a soft ferrimagnet, which is consistent with the thermomagnetic irreversibility and magnetic susceptibility behavior. Interestingly, the experimentally determined effective magnetic moment of ∼1.4 μ_B at 5 K is significantly smaller than the expected value of 3 μ_B estimated assuming an antiparallel alignment of the spins of Cu(II) and Cr(III). Significant spin canting may account for the small magnetic moment. Such an anomalously small magnetization is similar to that of $CuCr_2O_4$ spinel showing a non-unidirectional spin canting behavior.

Introduction

The widespread occurrence of ABO_3 and related oxides with the perovskite structure is attributed in large part to the flexibility of the corner-sharing BO_6 octahedral framework.[1] Since the A cation occupies the relatively large 12-oxygen-coordinated cubo-octahedral interstice created by corner-sharing octahedra, an octahedral tilting distortion occurs when the size of A cation is not optimal for the octahedral framework. Thus, if the A cation is too small, A−O bonding stabilizes structures having a smaller oxygen coordination environment about the A cation. Interesting examples include the $AA'_3B_4O_{12}$ perovskite family, where A generally represents a large cation and A′ is Cu(II) or Mn(III).[2,3] A significant tilting of the BO_6 octahedral network creates an essentially square-planar coordination for the stabilization of the smaller Cu(II) or Mn(III) ions on the A′ site. The fact that both Cu(II)(d^9) and Mn(III)(d^4) are Jahn−Teller cations with a strong preference for square-planar coordination rationalizes this unusual modification of the perovskite structure.

A magnetic interaction between cations occupying crystallographically different sites has been widely investigated in AB_2O_4 spinel oxides with d^n transition-metal ions on both tetrahedral A and octahedral B sites.[4] The competing exchange between A-site cations, B-site cations, and A−B-site cations leads to interesting magnetic behaviors. Beside typical ferromagnetic and ferrimagnetic interactions, several unusual spin alignments, such as triangular spin arrangements,[5] helical spin configurations,[6] and hexagonal spin clusters[7] are proposed in spinel systems. Although diverse magnetic interactions between the B-site cations have been investigated extensively in normal ABO_3 perovskite materials,[8] an interaction between localized d electrons for cations on both the A and B sites is less commonly reported. The inappropriateness of small d^n transition-metal ions for the relatively large size of the A site may account for this paucity of examples. Reports of magnetic interactions between A- and B-site cations concern mainly those perovskites having rare-earth cations on the A sites.

The magnetic properties of $AA'_3B_4O_{12}$ oxides with Cu(II) and/or Mn(III) cations occupying the A′ sites have been

* To whom correspondence should be addressed. E-mail: shbyun@khu.ac.kr or john.parise@sunysb.edu.
† Kyung Hee University.
‡ State University of New York, Stony Brook.
§ The Ohio State University.
|| KRISS.

(1) Megaw, H. D. *Nature* **1945**, *155*, 484.
(2) Chenavas, J.; Joubert, J. C.; Marezio, M.; Bochu, B. *J. Solid State Chem.* **1975**, *14*, 25.
(3) Deschizeaux, M. N.; Joubert, J. C.; Vegas, A.; Collomb, A.; Chenavas, J.; Marezio, M. *J. Solid State Chem.* **1976**, *19*, 45.
(4) Bonnenberg, D.; Boyd, E. L.; Calhoun, B. A.; Folen, V. J.; Gräper, W.; Greifer, A. P.; Kriessman, C. J.; Lefever, R. A.; McGuire, T. R.; Paulus, M.; Stauss, G. H.; Vautier, R.; Wijn, H. P. J. *Landolt-Börnstein: Numerical Data and Functional Relationships in Scienec and Technology*, New Series, Group III; Hellwege, K. H., Ed.; Springer-Verlag: Berlin, 1970; Vol. 4b.
(5) Prince, E. *Acta Crystallogr.* **1957**, *10*, 554.
(6) Hastings, J. M.; Corliss, L. M. *J. Phys. Soc. Jpn.* **1962**, *17*, 43.
(7) Lee, S.-H.; Broholm, C.; Ratcliff, W.; Gasparovic, G.; Huang, Q.; Kim, T. H.; Cheong, S.-W. *Nature* **2002**, *418*, 856.
(8) Goodenough, J. B.; Gräper, W.; Holtzberg, F.; Huber, D. L.; Lefever, R. A.; Longo, J. M.; McGuire, T. R.; Methfessel, S. *Landolt-Börnstein: Numerical Data and Functional Relationships in Sciene and Technology*, New Series, Group III; Hellwege, K. H., Ed.; Springer-Verlag: Berlin, 1970; Vol. 4a.

10.1021/cm050397b CCC: $30.25
Published on Web 06/02/2005

explored in relatively few systems. These compounds are of interest though because the topology of the magnetic network is such that A′−O−B interactions are competitive with the B−O−B and/or A′−O−A′ interactions. For instance, $(YCu_{2.3}Mn_{0.7})Mn_4O_{12}$ shows that Mn(III)−Mn(IV) on the B sites are coupled ferromagnetically, while the exchange of Cu(II)−Mn(IV) on the A′ and B sites is antiferromagnetic.[9] Similar magnetic interactions observed in $(CaCu_{2.5}Mn_{0.5})Mn_4O_{12}$ and $(NaMn_3)Mn_4O_{12}$ are correlated to their colossal magnetoresistance behaviors.[10,11] However, the magnetic properties of these compounds are governed by the competition between double-exchange and superexchange interactions between Mn(III)/Mn(IV) cations on the octahedral sublattice. In contrast, a strong Cu(II)−O−B(IV,V) ↔ Cu(III)−O−B(III,IV) charge transfer resulting in a metallic and Pauli-paramagnetic character is observed in $NaCu_3Ru_4O_{12}$, $CaCu_3Ru_4O_{12}$,[12] and $CaCu_3Cr_4O_{12}$.[13]

Through the study of $AA'_3B_2B'_2O_{12}$ compositions where the B and B′ ions are well ordered and B′ is a diamagnetic ion, it may be possible to simultaneously inhibit the electron delocalization that leads to either Pauli-paramagnetism or double-exchange ferromagnetism while at the same time diminishing the strength of the superexchange interactions on the octahedral sublattice, thereby enabling a direct study of the A′−O−B superexchange interactions. In this study we describe the synthesis and characterization of $CaCu_3Cr_2Sb_2O_{12}$ where the magnetic Cr(III) ions are diluted by nonmagnetic Sb(V) ions in an ordered manner so that Cr(III)−Cr(III) superexchange coupling in the octahedral network is sufficiently reduced in comparison with that of Cu(II)−Cr(III) on the different sites. This strategy was based on the recent success of high-pressure synthesis of $CaCu_3Ga_2B_2O_{12}$ (B = Sb and Ta) perovskites exhibiting simultaneous ordering on both A and B sites.[14] The magnetic measurements of $CaCu_3Cr_2Sb_2O_{12}$ reveal behavior typical of a soft ferrimagnet, suggesting that as designed the Cu(II)−Cr(III) interactions are dominant rather than the Cr(III)−Cr(III) interactions. Interestingly the observed magnetic moment at low temperature was significantly smaller than the expected value. We speculate that the reduced magnetic moment is mainly due to the spin canting, which suggests similarities with the spinel $CuCr_2O_4$ system.

Experimental Section

For the synthesis of $CaCu_3Cr_2Sb_2O_{12}$, a stoichiometric mixture of dried $CaCO_3$, CuO, Cr_2O_3, and Sb_2O_5 was calcined at 850 °C in air for 10 h with intermittent grinding. The reacted oxide mix was then thoroughly reground and sealed in a Au capsule with an inside diameter of 3.2 mm and a wall thickness of 0.1 mm. A high pressure−high temperature (HPHT) reaction was applied at 10 GPa and 1100 °C for 1 h, followed by temperature quenching and slow decompression using the 2000-ton uniaxial split-sphere apparatus (USSA 2000).[15] The sample was then recovered from the Au capsule as a dense pellet of about 50 mm^3.

The formation of a perovskite-related phase was initially confirmed by X-ray powder diffraction, taken on the sample pellet after recovery from the HPHT reaction using a general area detector diffraction system (GADDS). All major peaks in the powder diffraction pattern could be indexed on the basis of a primitive cubic cell with an approximate cell dimension $a \approx 7.46$ Å. Intensity data suitable for Rietveld structure refinement were collected on a rotating anode source installed diffractometer (MacScience Model M18XHF) with X-ray source of 40 kV and 300 mA. The use of a curved-crystal graphite monochromator ensured that only Cu Kα radiation reached the detector. The data were collected with a step-scan procedure in the range $2\theta = 10-120°$ with a step width of 0.02° and a step time of 1 s. The unit-cell parameter was derived by least-squares refinement using the powder diffraction data. Because of a limited quantity of sample recovered after the high-pressure treatment, the diffraction intensity data were obtained for a small amount of powder sample dispersed on a glass plate with absolute ethanol. The refinement of structural and instrumental parameters was carried out using the Rietveld analysis program RIETAN-2000.[16]

Elemental analysis using the energy-dispersive X-ray (EDX) emission technique gave the stoichiometric composition within experimental errors. Electrical resistivity was measured using a standard four-probe technique on the polycrystalline sample obtained from the high-pressure synthesis. The temperature dependence of the magnetic susceptibility was investigated on a powder sample from 5 to 300 K in an applied magnetic field of 5 kG using a Quantum Design MPMS-5 SQUID magnetometer. DC magnetization measurements were made after cooling the sample both in zero magnetic field (zero field cooled) and in the measured field (field cooled). Isothermal magnetization curves were recorded up to 50 kG after cooling the sample in zero magnetic field to the respective temperatures.

Results and Discussion

Attempts to synthesize $CaCu_3Cr_2Sb_2O_{12}$ at ambient pressure were unsuccessful. Instead multiple phases containing Sb_2O_5 were obtained after ambient pressure heat treatments. The initial X-ray powder diffraction pattern collected on a GADDS showed that $CaCu_3Cr_2Sb_2O_{12}$ was isolated as the dominant phase after temperature quenching the sample from high-pressure conditions. Some peaks attributed to impurities ($I/I_{max} < 0.05$) were present in repeated reactions carried out at different temperature and pressure conditions. The dominant phase however could be indexed on a primitive cubic cell with approximate cell parameter $a \approx 7.5$ Å, about twice that expected for ABO_3 aristotype perovskite structure. Further, the existence of strong (111) reflection in the X-ray diffraction (XRD) pattern was noted. For cubic $A_2BB'O_6$ or $AA'BB'O_6$ double perovskites, the presence and relative intensity of the (111) reflection is a very sensitive indicator to the degree of ordering of cations over the octahedral B sites. As observed in other members of the $CaCu_3B_2B'_2O_{12}$

(9) Bochu, B.; Joubert, J. C.; Collomb, A.; Ferrand, B.; Samaras, D. *J. Magn. Magn. Mater.* **1980**, *15*−*18*, 1319.
(10) Sanchez-Benitez, J.; Alonso, J. A.; Martinez-Lope, M. J.; Casais, M. T.; Martinez, J. L.; De Andres, A.; Fernandez-Diaz, M. T. *Chem. Mater.* **2003**, *15*, 2193.
(11) Prodi, A.; Gilioli, E.; Gauzzi, A.; Licci, F.; Marezio, M.; Bolzoni, F.; Huang, Q.; Santoro, A.; Lynn, J. W. *Nature Mater.* **2004**, *3*, 48.
(12) Labeau, M.; Bochu, B.; Joubert, J. C.; Chenavas, J. *J. Solid State Chem.* **1980**, *33*, 257.
(13) Subramanian, M. A.; Marshall, W. J.; Calvarese, T. G.; Sleight, A. W. *J. Phys. Chem. Solids* **2003**, *64*, 1569.
(14) Byeon, S.-H.; Lufaso, M. W.; Parise, J. B.; Woodward, P. M.; Hansen, T. *Chem. Mater.* **2003**, *15*, 3798.
(15) Liebermann, R. C.; Wang, Y. *High-Pressure Research: Application to Earth and Planery Sciences*; Terrapub: Tokyo, 1992.
(16) Izumi, F.; Murata, H.; Watanabe, N. *J. Appl. Crystallogr.* **1987**, *20*, 411.

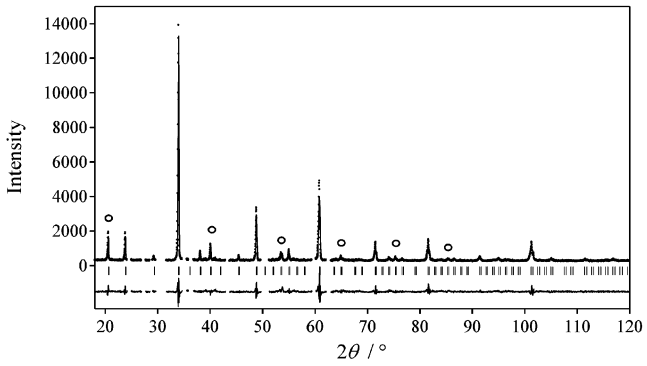

Figure 1. Observed X-ray powder diffraction data (dotted line) along with the calculated diffraction pattern (solid line) obtained from Rietveld refinement of $CaCu_3Cr_2Sb_2O_{12}$. Regions of the pattern containing impurity peaks are excluded. At the bottom of the figure, the difference plot ($I_{obs} - I_{calc}$) is shown on the same scale. Vertical bars on the bottom indicate the positions of allowed Bragg reflections. Open circles represent the reflections indicative of long-range Cr:Sb order.

family, an ordered arrangement of the octahedral B and B′ cations changes the space group symmetry from $Im\bar{3}$ to $Pn\bar{3}$.[17] Intensity data for $CaCu_3Cr_2Sb_2O_{12}$ obtained by step-scan procedure were quite similar to that of ordered $CaCu_3Ga_2Sb_2O_{12}$,[14] thereby implying it is isostructural with this compound.

Extinction conditions also supported the space group assignment of $Pn\bar{3}$, consistent with an ordered perovskite structure in the $a^+a^+a^+$ Glazer tilt system.[18−20] Accordingly, the atomic positions of ordered perovskite $CaCu_3Ga_2Sb_2O_{12}$ were used in the initial stage of structure refinement for $CaCu_3Cr_2Sb_2O_{12}$. The positions of the impurity peaks did not correspond to either X-ray patterns obtained after ambient pressure heat treatments nor those expected for likely minority phases, such as CuO, Cr_2O_3, CrO_2, and $CaCrO_3$. Attempts to identify the impurity phase(s) were unsuccessful, and these trace impurities may also correspond to pressure stabilized phases. When the regions corresponding to the strongest peaks from the impurity phase(s) were excluded from subsequent Rietveld refinement, the residual fit parameter was noticeably reduced. During the refinements we assumed the stoichiometry $CaCu_3Cr_2Sb_2O_{12}$ and Cr/Sb distributed over the B sites. The requirements of stoichiometry and charge balance impose constraints, which can be incorporated straightforwardly into the Rietveld refinement.

The observed diffraction data, as well as the calculated pattern and difference curve from the Rietveld refinement of $CaCu_3Cr_2Sb_2O_{12}$, are shown in Figure 1. The strong and systematic reflections marked by the open circles are attributed to an ordered structure. Crystallographic data, including refined atomic coordinates and isotropic displacement parameters are listed in Table 1. The ordering between Cr and Sb atoms is essentially complete over the octahedral B sites. A trial to refine the occupancy of Cr and Sb atoms resulted in 0.050(5) of occupancy factor for the 4b (0, 0, 0) and 4c (0.5, 0.5, 0.5) sites, respectively. However, no remarkable change was induced in the goodness-of-fit parameters. Thus, there was no compelling evidence for disorder, although it was difficult to completely rule out a small amount of disorder.

Table 1. Structure Refinement Results for $CaCu_3Cr_2Sb_2O_{12}$

compound	$CaCu_3Cr_2Sb_2O_{12}$
R_{wp} (%)	9.65
R_p (%)	7.37
R_E (%)	5.09
R_F (%)	9.16
space group	$Pn\bar{3}$
a (Å)	7.4605(4)

Atomic Positions

atoms	g[a]	x	y	z	U_{iso} (Å^2)
Ca	1.0	0.25	0.25	0.25	0.002(6)
Cu	1.0	0.25	0.75	0.75	0.007(2)
Sb	1.0	0.0	0.0	0.0	0.0046(6)
Cr	1.0	0.5	0.5	0.5	0.0015(9)
O	1.0	0.2589(8)	0.422(1)	0.550(1)	0.015(2)

[a] The site occupancies of all atoms were fixed to 1.0.

Table 2. Selected Bond Lengths and Bond Angles for $CaCu_3Cr_2Sb_2O_{12}$

bond distances (Å)	
Ca−O (×12)	2.585(8)
Cu−O (×4)	1.973(7)
Cr−O (×6)	1.926(6)
Sb−O (×6)	2.048(6)
bond angles (deg)	
O−Cu−O (×2)	98.0(7)
O−Cu−O (×2)	82.0(7)
O−Cr−O (×6)	88.0(5)
O−Cr−O (×6)	92.0(5)
O−Sb−O (×6)	87.9(5)
O−Sb−O (×6)	92.1(5)
Cr−O−Sb	139.5(4)
Cu−O−Cr	112.1(3)
Cu−O−Sb	107.0(3)

Selected interatomic distances and angles are listed in Table 2. The structure of $CaCu_3Cr_2Sb_2O_{12}$, shown in Figure 2, is quite similar to those of other members of ordered $CaCu_3B_2B'_2O_{12}$ family.[14] The considerable size mismatch and differences in bonding requirements for Ca(II) and Cu(II) leads to ordering of these elements in the A sites and to significant deviation of Cr−O−Sb angle (139.5°) from 180° by the tilting of CrO_6 and SbO_6 octahedra. Copper is at the center of a slightly distorted square-planar site with four next-nearest oxygen atoms at 2.86 Å and four additional oxygens at 3.31 Å. By comparison of the angles of O−Cr−O and O−Sb−O bonds, the octahedra are quite regular, consistent with the idea of tilting of essentially rigid octahedra. In general the bond distances and angles are very similar to those previously obtained from neutron powder diffraction data for $CaCu_3Ga_2Sb_2O_{12}$.[14] The bond valence is commonly expressed as $v_{ij} = \exp[(R_{ij} - d_{ij})/b]$, where R_{ij} and d_{ij} are the bond valence parameter and bond length, with a universal b constant of 0.37.[21] The bond valence sums calculated on the basis of refined bond distances are 2.26 for Ca, 2.05 for Cu, 3.24 for Cr, 4.80 for Sb, and 2.04 for O, respectively. Here we see that the calculated valences are close to the expected

(17) Howard, C. J.; Kennedy, B. J.; Woodward, P. M. *Acta Crystallogr.* **2003**, *B59*, 463.
(18) Glazer, A. M. *Acta Crystallogr.* **1972**, *B28*, 3384.
(19) Woodward, P. M. *J. Appl. Crystallogr.* **1997**, *30*, 206.
(20) Aleksandrov, K. S.; Misjul, S. V. *Sov. Phys. Crystallogr.* **1981**, *26*, 612.
(21) Brown, I. D. *The Chemical Bond in Inorganic Chemistry. The Bond Valence Model*, IUCr Monograph on Crystallography; Oxford University Press: Oxford; 2002; Vol. 12.

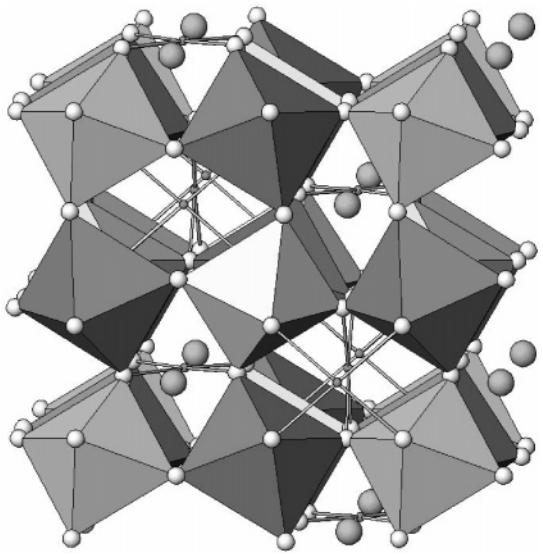

Figure 2. Structure of $CaCu_3Cr_2Sb_2O_{12}$. The origin of the unit cell is at the Sb atom centered on the white octahedron. Large shaded and small dark spheres represent Ca and Cu atoms, respectively. Shaded octahedra and white spheres represent CrO_6 units and oxygen atoms, respectively. Only Cu−O bonds are represented by double lines to show four-coordinated CuO_4 arrangement.

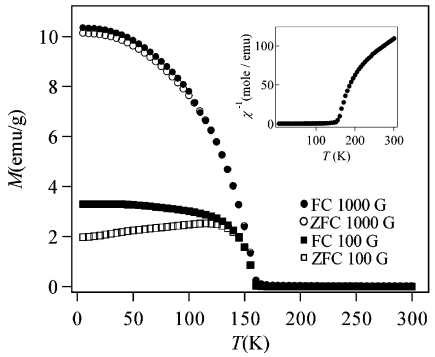

Figure 3. Field-cooled and zero-field-cooled magnetization of $CaCu_3Cr_2Sb_2O_{12}$ measured at 100 and 1000 G. Inset shows the temperature dependence of field-cooled inverse molar magnetic susceptibility measured at 5000 G.

values and support the accuracy of the structure determination.

The measurement of the electrical conductivity showed that $CaCu_3Cr_2Sb_2O_{12}$ is an insulator. Its room-temperature resistance was too high to be measured with our instruments. Figure 3 shows the temperature dependence of field-cooled magnetization M_{FC} and zero-field-cooled magnetization M_{ZFC} of $CaCu_3Cr_2Sb_2O_{12}$ at different magnetic fields. An abrupt increase in the magnetization occurs below ~160 K, indicating the presence of a ferromagnetic transition. Magnetic impurities could drive the ferromagnetic transition at similar temperature. However, the starting magnetic materials CuO and Cr_2O_3 order antiferromagnetically upon cooling.[22] The ferromagnetic to paramagnetic transition temperature of CrO_2, which is the most plausible oxide, is in the range of 389−398 K.[23,24] The orthorhombic perovskite $CaCrO_3$ also exhibits parasitic ferromagnetism below 90 K.[25] The lack of a known compound in the phase diagram with a ferromagnetic or ferrimagnetic ordering temperature near 160 K lends strong support to our claim that the observed ferro- or ferrimagnetic transition can be ascribed to $CaCu_3Cr_2Sb_2O_{12}$.

In Figure 3, no difference between M_{FC} and M_{ZFC} is observed when measured at 1000 G. In contrast, the zero-field-cooled magnetization curve measured at 100 G exhibits a broad maximum with M_{ZFC} slowly increasing up to ~120 K. An irreversible thermomagnetic behavior is frequently observed for magnetically ordered systems, a sharp peak (a cusp) around the Curie temperature (T_c) and a drastic decrease in M_{ZFC} below T_c being observed for highly anisotropic systems.[26,27] For instance, the ferromagnetic perovskite-oxide $SrRuO_3$ and the ferromagnetic spinel-oxide $MnCo_2O_4$, which have large magnetic anisotropy, show a sharp peak in $M_{ZFC}(T)$ curves and large thermomagnetic irreversibility below T_c when measured with small dc magnetic fields.[28,29] On the other hand, a broad maximum is observed in $M_{ZFC}(T)$ for soft magnetic materials and only a small decrease of magnetization is observed below T_c when measured with small magnetic field. The peak in M_{ZFC} is broadened with increasing applied field strength. Soft magnetic materials, such as $NiFe_2O_4$ ferrimagnetic spinel[30] and $La_{2/3}Ca_{1/3}MnO_3$ ferromagnetic perovskite,[31] for example, show an irreversibility of field-cooled and zero-field-cooled magnetization behaviors when measured with low magnetic fields. However, the difference between field-cooled and zero-field-cooled magnetization is much less in soft magnetic systems when compared with the large difference observed for hard systems.[32] Accordingly, observation of a broad maximum in $M_{ZFC}(T)$ and weak thermomagnetic irreversibility, even at a weak magnetic field as shown in Figure 3, suggests that $CaCu_3Cr_2Sb_2O_{12}$ ordered perovskite is a soft magnet. The inverse magnetic susceptibility curve shown in the inset of Figure 3, is similar to those of typical ferrimagnetic materials and shows no linear range that can be fitted to a Curie−Weiss law up to 300 K.

The isostructural oxide $CaCu_3Ti_4O_{12}$, where only A sites are occupied by the magnetic Cu(II)(d^9) cations, antiferromagnetically orders via superexchange between (111) Cu−O planes below 27 K, but the projections of three Cu(II) spins on a (111) plane are not collinear but at 120° angles to each other.[33] Such a noncollinearity of the spins was attributed to spin−orbit coupling.[34] In ordered $A_2BB'O_6$ perovskites involving diamagnetic B′ cations arranged in alternate octahedral sites, there are two competing interactions between magnetic B cations; a 180° B−O−B′−O−B σ superexchange and a 90° B−O−O−B π superexchange. An

(22) Nagamiya, T.; Yoshida, K.; Kubo, R. *Adv. Phys.* **1955**, *4*, 1.
(23) Darnell, F. J.; Cloud, W. H. *Bull. Soc. Chim. Fr.* **1965**, 1164.
(24) Stoffel, A. M. *J. Appl. Phys.* **1969**, *40*, 1238.
(25) Goodenough, J. B.; Longo, J. M.; Kafalas, J. A. *Mater. Res. Bull.* **1968**, *3*, 471.
(26) Kumar, P. S. A.; Joy, P. A.; Date, S. K. *J. Phys. Condens. Matter* **1998**, *10*, L487.
(27) Pechev, S.; Chevalier, B.; Laffargue, D.; Darriet, B.; Roisnel, T.; Etourneau, J. *J. Magn. Magn. Mater.* **1999**, *191*, 282.
(28) Kumar, P. S. A.; Joy, P. A.; Date, S. K. *Physica B* **1999**, *269*, 356.
(29) Joy, P. A.; Date, S. K. *J. Magn. Magn. Mater.* **2000**, *210*, 31.
(30) Anil, K. P. S.; Shrotri, J. J.; Kulkarni, S. D.; Deshpande, C. E.; Date, S. K. *Mater. Lett.* **1996**, *27*, 293.
(31) Anil, K. P. S.; Alias, J. P.; Date, S. K. *J. Mater. Chem.* **1998**, *8*, 1219.
(32) Kumar, P. S. A.; Joy, P. A.; Date, S. K. *J. Phys.: Condens. Matter* **1998**, *10*, 11049.
(33) Collomb, A.; Samaras, D.; Bochu, B.; Joubert, J. C. *Phys. Stat. Sol. A* **1977**, *41*, 459.
(34) Lacroix, C. *J. Phys. C* **1980**, *13*, 5125.

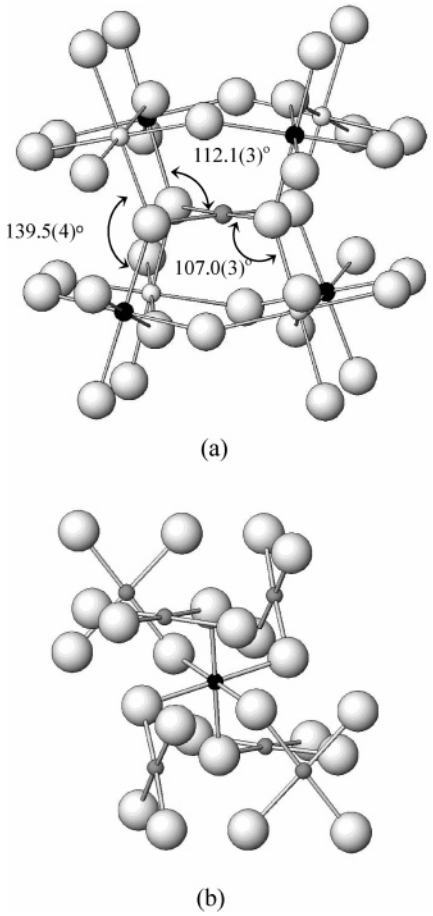

Figure 4. Interconnection networks of CuO_4 square planes, CrO_6 octahedra, and SbO_6 octahedra. (a) Cu atom and (b) Cr atom is located at the center. Small shaded spheres, small black spheres, small white spheres, and large white spheres represent Cu, Cr, Sb, and O atoms, respectively.

antiferromagnetic coupling via the π-superexchange mechanism is often predominant in oxides. For example, ordered Cr(III)(d^3) double perovskite oxide Sr_2CrSbO_6 undergoes antiferromagnetic ordering at 9 K.[35] Sr_2FeSbO_6 also orders antiferromagnetically (A type) at 35−40 K, and the dominant coupling pathway is thought to be π superexchange.[36] If we consider the strong deviation of Cr−O−Sb angle (139.5°) from 180° (Table 2), the dominant magnetic coupling in the octahedral network of $CaCu_3Cr_2Sb_2O_{12}$ can be similarly expected to be antiferromagnetic π superexchange via Cr(III)(t_{2g})−O(2p)−O(2p)−Cr(III)(t_{2g}) pathways. However, the magnetic interactions in $CaCu_3Cr_2Sb_2O_{12}$ are more complex than those in $CaCu_3Ti_4O_{12}$, Sr_2CrSbO_6, and Sr_2FeSbO_6 perovskites. Thus the competing coupling between the magnetic A-site Cu(II) ($S = {}^1/_2$) and B-site Cr(III) ($S = {}^3/_2$) ions may also influence the overall magnetic properties. The interconnection between networks of magnetic Cu(II) and Cr(III) cations in $CaCu_3Cr_2Sb_2O_{12}$ are schematically illustrated in Figure 4. Compared with the long distance Cu(II)−Cu(II) and Cr(III)−Cr(III) magnetic interactions, the Cu(II)−Cr(III) superexchange interaction could be stronger because of significant tilting of CrO_6 and SbO_6 octahedra. This analysis together with the results shown in Figure 3

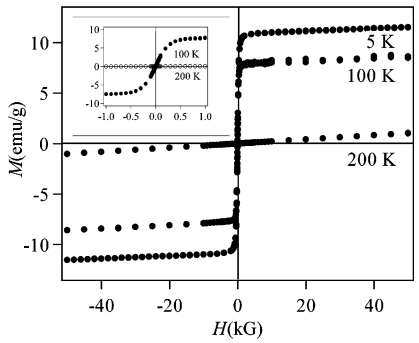

Figure 5. Magnetization loop for $CaCu_3Cr_2Sb_2O_{12}$ acquired at different temperatures. Inset shows the magnetization curve at low magnetic field ($-1 < H < 1$ kG).

indicates that an exchange interaction between A-site Cu(II) and B-site Cr(III) cations dominates over possible antiferromagnetic couplings between Cu(II)−Cu(II) ions or Cr(III)−Cr(III) ions and induces a net spontaneous magnetic moment below ~160 K. In light of the low magnetic ordering temperatures of $CaCu_3Ti_4O_{12}$ (27 K), Sr_2CrSbO_6 (9 K), and Sr_2FeSbO_6 (35 K), the relatively high magnetic ordering temperature strongly supports our hypothesis that the Cu−O−Cr superexchange pathway is dominant.

Isothermal magnetization measurements for $CaCu_3Cr_2Sb_2O_{12}$ were carried out to elucidate the origin of the magnetic interaction and to search for a possible magnetic hysteresis loop which usually occurs in hard ferromagnets. As shown in the dc magnetization $M(T,H)$ curves of Figure 5, no significant hysteresis, at least in high fields, is observed. This is further proof for the assertion that $CaCu_3Cr_2Sb_2O_{12}$ is a soft ferrimagnet, as expected from thermomagnetic irreversibility and magnetic susceptibility behaviors (Figure 3). This figure also supports the claim that the magnetic signals are not ascribed to a magnetic impurity but to the bulk property of $CaCu_3Cr_2Sb_2O_{12}$. The saturation effects are seen beyond $H \approx 1$ kG at low temperature and the coercivity (H_c) is close to 200 G at 100 K (inset of Figure 5). One interesting feature is that an effective magnetic moment of ~1.4 μ_B is deduced from the spontaneous magnetization value at 5 K in Figure 5. Although we assume that the moments of A-site Cu(II) and B-site Cr(III) are antiparallel to each other, this value is significantly smaller than that expected, 3 μ_B. To interpret this result, it is instructive to refer to a density functional calculation for $CaCu_3Mn_4O_{12}$,[37] which shows antiparallel alignment of Cu(II) and Mn(IV) spins yielding 9 μ_B net spin moment, consistent with the formal spins. To a first approximation, a canted arrangement of two spins would explain a significantly smaller magnetic moment for $CaCu_3Cr_2Sb_2O_{12}$.

Spin canting is often observed in perovskite systems where a double-exchange mechanism can give a net ferromagnetic moment.[38] In contrast, strong differences in spontaneous magnetization are not common in systems, such as $CaCu_3Cr_2Sb_2O_{12}$, where double-exchange interactions are absent. Rather, the observed behavior in $CaCu_3Cr_2Sb_2O_{12}$ is similar to that observed for Cu(II)Cr(III)$_2O_4$ spinel. The magnetic

(35) Blasse, G. *J. Appl. Phys.* **1965**, *36*, 879.
(36) Cussen, E. J.; Vente, J. F.; Battle, P. D.; Gibb, T. C. *J. Mater. Chem.* **1997**, *7*, 459.
(37) Weht, R.; Pickett, E. *Phys. Rev. B* **2001**, *65*, 014415.
(38) Zener, C. *Phys. Rev.* **1951**, *82*, 403.

moment observed for this oxide was 0.4−0.8 μ_B/mol below T_c (∼135 K), which is much smaller than the expected value 5 μ_B/mol.[39] A probable explanation is that Cr(III) ions are divided into two sets with spins directed at an angle to each other and with the spins of Cu(II) ions directed antiparallel to the resultant, which is consistent with a triangular spin configuration model.[40] In the $CuCr_2O_4$ lattice, the Cu(II) ions occupy tetrahedral sites, but the Cu−O−Cu bond angles of 103 and 123° show a tendency toward square coordination and the Cu−O−Cr bond angle is close to 116°.[5] A ferrimagnetic spiral spin configuration is also proposed to explain an anomalously small value of spontaneous magnetization particularly in spinel system.[41]

In the structure of $CaCu_3Cr_2Sb_2O_{12}$, the tilting of four CrO_6 octahedra connected to a CuO_4 square plane are not unidirectional (Figure 4a). Six CuO_4 square planes are connected to each CrO_6 octahedron with a 112° angle of the Cu−O−Cr bond. The planes of three opposite CuO_4 pairs are nearly orthogonal to one another, but the planes of two CuO_4 squares in the opposite side are not parallel (Figure 4b). Because of such structural characteristics, the spin alignments in $CaCu_3Cr_2Sb_2O_{12}$ lattice would be more complicated than those for spinel system. Although the lack of neutron diffraction data made it difficult to refine the canting angle, we suggest that strongly canted spins would induce a small spontaneous magnetization. The neutron diffraction study of this compound is in progress.

Conclusions

We have successfully synthesized a new magnetic perovskite-type oxide $CaCu_3Cr_2Sb_2O_{12}$ under high-pressure and high-temperature conditions. Rietveld refinement using XRD data revealed that Cr and Sb atoms are ordered over the octahedral sites. A soft ferrimagnetic behavior of $CaCu_3Cr_2Sb_2O_{12}$ seems to be largely associated with Cu(II)−Cr(III) superexchange interaction. The reduced value of spontaneous magnetization suggests that the alignments of each spin would be canted. The magnetic interactions between A- and B-site cations are well established for the perovskites having rare-earth A cations but, to the best of our knowledge, not actively investigated for the perovskites having d^n transition-metal A cations. Further investigations of ordered $ACu_3B_2B'_2O_{12}$ or $AMn_3B_2B'_2O_{12}$ family, where B′ is nonmagnetic cation, would thus provide in-depth understanding on a complicated magnetic interaction between localized d electrons on the A and B sites of the perovskite structure.

Acknowledgment. J.B.P. acknowledges support of the NSF through Grants DMR-0095633 and EAR 0125094. P.M.W. acknowledges support of the NSF through its Chemical Bonding Centers Program, Grant No. 0434567. Research carried out at Kyung Hee University was supported by the KOSEF through Grant R01-2004-000-10610-0.

CM050397B

(39) McGuire, T. R.; Howard, L. N.; Smart, J. D. *Ceram. Age* **1952**, *60*, 22.
(40) Yafet, Y.; Kittel, C. *Phys. Rev.* **1952**, *87*, 290.
(41) Kaplan, T. A.; Dwight, K.; Lyons, D.; Menyuk, N. *J. Appl. Phys.* **1961**, *32*, 135.